J Polym Res (2007) 14:359–372
DOI 10.1007/s10965-007-9118-6

# Synthesis and properties of *ortho*-linked aromatic poly(ester-amide)s and poly(ester-imide)s bearing 2,3-bis(benzoyloxy)naphthalene units

**Wenjeng Guo · Wen-Tsuen Leu · Sheng-Huei Hsiao**

Received: 16 March 2007 / Accepted: 8 May 2007 / Published online: 12 June 2007


**Abstract** Two new naphthalene-ring-containing bis(ester-amine)s, 2,3-bis(4-aminobenzoyloxy)naphthalene (*p*-**2**) and 2,3-bis(3-aminobenzoyloxy)naphthalene (*m*-**2**), were prepared from the condensation of 2,3-dihydroxynaphthalene with 4-nitrobenzoyl chloride and 3-nitrobenzoyl chloride, respectively, followed by catalytic hydrogenation. The novel aromatic poly(ester-amide)s and poly(ester-imide)s having 2,3-linked bis(benzoyloxy)naphthalene units have been synthesized from the polycondensation reactions of bis(ester-amine)s (*p*-**2** and *m*-**2**) or an equimolar mixture of 4,4′-oxydianiline and *p*-**2** or *m*-**2** with various aromatic dicarboxylic acids and dianhydrides. The synthesis of the poly(ester-amide)s was achieved by the phosphorylation polyamidation reaction by means of triphenyl phosphate, and the synthesis of the poly(ester-imide)s included ring-opening polyaddition to give poly(amic acid)s followed by chemical imidization to polyimides. Most of the poly(ester-amide)s were readily soluble in various organic solvents. Six poly(ester-amide)s and two poly(ester-imide)s derived from less rigid diacids and dianhydrides, respectively, were amorphous and could be solution-cast into transparent and tough films with good mechanical properties. Most of the poly(ester-amide)s displayed discernible glass-transition temperatures ($T_g$s) between 192 and 223 °C in the DSC traces. All of the poly(ester-imide)s, except for one sample, showed clear $T_g$ values between 225 and 265 °C by DSC. These poly(ester-imide)s showed excellent thermal stability with 10 wt% loss temperatures above 460 °C in nitrogen or air.

**Keywords** Naphthalene units · Ortho links · Bis(ester-amine)s · Poly(ester-amide)s · Poly(ester-imide)s

W. Guo
Department of Chemical Engineering,
National Taipei University of Technology,
1 Chunghsiao East Road, 3rd Section,
Taipei 100, Taiwan, Republic of China

W.-T. Leu · S.-H. Hsiao (✉)
Department of Chemical Engineering, Tatung University,
40 Chungshan North Road, 3rd Section,
Taipei 104, Taiwan, Republic of China
e-mail: shhsiao@ttu.edu.tw

## Introduction

Aromatic polyamides and polyimides have been categorized as the high-performance polymeric materials with several useful properties such as outstanding thermal stability, high radiation and chemical resistance, low flammability, and excellent mechanical properties [1–6]. However, these polymers usually encounter processing difficulties due to their high glass-transition ($T_g$) or melting temperatures and limited solubility in common organic solvents. Therefore, a lot of efforts have been attempted to improve the processing characteristics of the relatively intractable polymers, while still maintaining the excellent thermal and mechanical properties. Those efforts include the introduction of flexible links [7–12], asymmetric units [13–16], bulky pendant groups [17–24], and kinked or non-coplanar structures [25–32] into the polymer chain. These modifications have lowered the $T_g$ or the melting temperatures and increased the solubility by reduction in crystallinity. A number of reports describe the syntheses of poly(ether-amide)s and poly(ether-imide)s based on diamines with ether linkages [33–36]. The incorporation of aryl-ether linkages generally imparts an enhanced solubility, processability, and toughness of the polymers without substantial diminution of thermal properties. It has been demonstrated that incorporation of both ether and naphthyl units

(especially using 2,3-linked naphthalene units) into the polymer backbones may enhance the solubility and processability of aromatic polyamides and polyimides without any significant reduction in thermal stability [37–43]. The introduction of a naphthalene ring into the polymer main chain is expected to lead to an increase in thermal stability as compared with the benzene ring, because of the contribution from the more rigid structure and higher resonance stabilization energy of the former. Another active line of research is to establish the influence of aromatic substitution patterns on the nature of aromatic polyamides and polyimides [44–47]. In continuing our interest in preparing easily processable high-performance polymers bearing naphthyl units, this present study deals with the synthesis and basic characterization of *ortho*-catenated aromatic poly(ester-amide)s and poly(ester-imide)s using the bis(ester-amine)s (*p*-**2** and *m*-**2**) bearing 2,3-bis(benzoyloxy) naphthalene unit as major diamine components. The presence of ester groups may provide the resulting polymers with higher flexibility in backbone and increased solubility. In addition, the formation of bent structures due to the presence of *ortho* links (2,3-disubstituted naphthalene units) will help prevent the extended close chain packing, and subsequently, the interchain interactions. Thus, the resulting polymers are expected to exhibit enhanced solubility and processability as compared to conventional aromatic polyamides and polyimides. The thermal properties of the poly(ester-amide)s and poly(ester-imide)s obtained from the bis(ester-amine) *p*-**2** are compared with those of structurally related poly(ether-amide)s and poly(ether-imide)s from 2,3-bis(4-aminophenoxy)naphthalene [37, 38].

## Experimental

### Materials

2,3-Dihydroxynaphthalene (from Acros), 4,4′-oxydianiline (from TCI), 4-nitrobenzoyl chloride (from Acros), 3-nitrobenzoyl chloride (from Acros) and 10% palladium on activated carbon (Pd/C, from Fluka) were used as received. Commercially available aromatic dicarboxylic acids such as terephthalic acid (**4a**, from Fluka), isophthalic acid (**4b**, from Wako), 4,4′-oxydibenzoic acid (**4c**, from TCI), 4,4′-hexafluoroisopropylidenedibenzoic acid (**4d**, from Chriskev), and 4,4′-sulfonyldibenzoic acid (**4e**, from New Japan Chemical Company) were used as received. Pyromellitic dianhydride (PMDA, **6a**) (Aldrich) was purified by recrystallization from acetic anhydride. 2,2-Bis(3,4-dicarboxyphenyl) hexafluoropropane dianhydride (6FDA, **6b**) (Hoechst Celanese) was heated *in vacuo* at 250 °C for 3 h prior to use. Commercially available anhydrous calcium chloride ($CaCl_2$) was dried *in vacuo* at 180 °C for 8 h prior to use. *N*-Methyl-2-pyrrolidone (NMP), *N,N*-dimethylformamide (DMF), *N,N*-dimethylacetamide (DMAc), and pyridine were purified by distillation under reduced pressure over calcium hydride and stored over 4 Å molecular sieves. Triphenyl phosphite (TPP) was also purified by distillation under reduced pressure.

### Monomer synthesis

#### *2,3-Bis(4-nitrobenzoyloxy)naphthalene (p-**1**) and 2,3-Bis (3-nitrobenzoyloxy)naphthalene (m-**1**)*

The dinitro-diester *p*-**1** was prepared by the condensation of 2,3-dihydroxynaphthalene with 4-nitrobenzoyl chloride. 2,3-Dihydroxynaphthalene (16 g, 0.1 mol), dissolved in 300 mL of dried DMAc, and triethylamine (30 mL, 0.22 mol) were mixed in a 1 L round-bottomed flask. A solution of 4-nitrobenzoyl chloride (39 g, 0.21 mol) in DMAc (100 mL) was then added dropwise over a period of about 1 h. After complete addition, the reaction mixture was stirred at 80 °C for 8 h. The reaction mixture was then poured into 1.5 L of water. The precipitate was collected by filtration, washed thoroughly with water and methanol, and dried. The crude product (43.6 g, 95% yield) was purified by recrystallization from DMF/$CH_3OH$ (150 mL/50 mL) to give 38.8 g (85% yield) of the pure dinitro-diester *p*-**1** as light yellowish crystals; mp=211 °C. IR (KBr) ($cm^{-1}$): 1,745 (C=O stretching), 1,523, 1,346 ($NO_2$ stretching), 1,275, 1,082 (C–O–C stretching). Elemental analysis, calculated for $C_{24}H_{14}N_2O_8$ (458.38): C, 62.89%; H, 3.08%; N, 6.11%. Found: C, 62.96%; H, 3.06%; N, 6.16%.

The dinitro-diester *m*-**1** was synthesized from 2,3-dihydroxynaphthalene and 3-nitrobenzoyl chloride according to a similar procedure. Pure *m*-**1** (83% yield) was obtained as 'off-white' crystals by recrystallization from DMF/$CH_3OH$ (100 mL/100 mL); mp=164 °C. IR (KBr) ($cm^{-1}$): 1,753 (C=O stretching), 1,535, 1,356 ($NO_2$ stretching), 1,261, 1,110 (C–O–C stretching). Elemental analysis, calculated for $C_{24}H_{14}N_2O_8$ (458.38): C, 62.89%; H, 3.08%; N, 6.11%. Found: C, 62.87%; H, 3.04%; N, 6.17%.

#### *2,3-Bis(4-aminobenzoyloxy)naphthalene (p-**2**) and 2,3-Bis (3-aminobenzoyloxy)naphthalene (m-**2**)*

The bis(ester-amine)s *p*-**2** and *m*-**2** were prepared by the catalytic hydrogenation of the dinitro-diester compounds *p*-**1**and *m*-**1**, respectively. A mixture of 32.4 g (0.07 mol) of the dinitro-diester compound *p*-**1** and 0.4 g of 10% Pd/C in 300 mL of DMAc was stirred at room temperature under a hydrogen atmosphere until the theoretical amount of

hydrogen was consumed. The time taken to reach this stage was about 3 d. The solution was filtered to remove the catalyst, and the obtained filtrate was poured into 1 L of stirred methanol to give a light grey crystalline product. The yield was 23.2 g (82%); mp=278 °C. IR (KBr) ($cm^{-1}$): 3,467, 3,373 ($NH_2$ stretching), 1,685 (C=O stretching), 1,282, 1,093 (C–O–C stretching). $^1$H NMR [400 MHz, DMSO-$d_6$, δ, ppm]: 7.94 (dd, *J*=8 Hz, 2 H), 7.91 (s, 2 H ), 7.70 (d, *J*=8 Hz, 4 H), 7.53 (dd, *J*=8 Hz, 2 H), 6.55 (d, *J*=8 Hz, 4 H), 6.13 (s, –$NH_2$, 4 H). $^{13}$C NMR (100 MHz, DMSO-$d_6$, δ, ppm): 164.43 (C=O), 154.51, 142.19, 132.18, 131.37, 127.61, 126.58, 121.13, 114.20, 113.12. Elemental analysis, calculated for $C_{24}H_{18}N_2O_4$ (398.42): C, 72.35%; H, 4.55%; N, 7.03%. Found: C, 72.47%; H, 4.63%; N, 6.97%.

The bis(ester-amine) *m*-**2** was synthesized from the dinitro-diester compound *m*-**1** as a light grey crystalline product with a 80% yield; mp=149 °C. IR (KBr) ($cm^{-1}$): 3,435, 3,354 ($NH_2$ stretching), 1,726 (C=O stretching), 1,294, 1,105 (C–O–C stretching). $^1$H NMR [400 MHz, DMSO-$d_6$, δ, ppm]: 8.02 (s, 2 H), 8.02 (d, *J*=8 Hz, 2 H), 7.61 (dd, *J*=8 Hz, 2 H ), 7.33 (s, 2 H), 7.23 (d, *J*= 8 Hz, 2 H), 7.16 (t, *J*=8 Hz, 2 H), 6.90 (d, *J*=8 Hz, 2 H), 5.43 (s, –$NH_2$, 4 H). $^{13}$C NMR (100 MHz, DMSO-$d_6$, δ, ppm): 165.12 (C=O), 149.38, 141.68, 131.68, 129.82, 129.05, 127.86, 127.10, 121.44, 119.94, 117.60, 114.89. Elemental analysis, calculated for $C_{24}H_{18}N_2O_4$ (398.42): C, 72.35%; H, 4.55%; N, 7.03%. Found: C, 72.40%; H, 4.59%; N, 7.07%.

## Synthesis of poly(ester-amide)s

A typical example of the phosphorylation polycondensation reaction employed for the preparation of the poly(ester-amide) *m*-**5j** is as follows. A mixture of 0.2391 g (0.60 mmol) of the bis(ester-amine) *m*-**2**, 0.1201 g (0.60 mmol) of 4,4′-oxydianiline, 0.3674 g (1.20 mmol) of 4,4′-sulfonyldibenzoic acid (**4e**), 0.2 g of calcium chloride, 2.0 mL of NMP, 0.5 mL of pyridine, and 1.2 mL of TPP was heated with stirring at 110 °C for 3 h. As the polycondensation proceeded, the solution gradually became viscous. The resulting highly viscous polymer solution was slowly poured onto 250 mL of stirred methanol, giving rise to a white, fiber-like precipitate which was collected by filtration, washed thoroughly with methanol and hot water and then dried at 100 °C in a vacuum oven. The yield was quantitative. The inherent viscosity of the obtained polymer *m*-**5j** was 0.68 dL/g, measured at a concentration of 0.5 g/dL in DMAc containing 5 wt% LiCl at 30 °C. The FT-IR spectrum (thin-film) exhibited characteristic absorptions at 3,332 (N–H stretching), 1,745 (ester C=O stretching), 1,662 (amide C=O stretching), 1,500 (N–H bending) and 1,249 and 1,099 $cm^{-1}$ (asymmetrical and symmetrical C–O–C stretching). All of the other poly(ester-amide)s were synthesized by using a similar procedure to that described above.

## Synthesis of poly(ester-imide)s

The synthesis of the poly(ester-imide) *m*-**8d** was used as an example to illustrate the general synthetic route used to produce the poly(ester-imide)s. To a solution of 0.2679 g (0.67 mmol) of the bis(ester-amine) *m*-**2** and 0.1346 g (0.67 mmol) of 4,4′-oxydianiline in 9.5 mL of $CaH_2$-dried DMAc in a 50-mL flask, 0.5971 g (1.34 mmol) of dianhydride 6FDA was added in one portion. Thus, the solid content of the solution is approximately 10 wt%. The mixture was stirred at room temperature overnight (for about 24 h) to afford a viscous poly(amic acid) solution. The inherent viscosity of the resultant poly(amic acid) *m*-**7d** was 0.65 dL/g, measured in DMAc at a concentration of 0.5 g/dL at 30 °C. The poly(amic acid) was subsequently chemically cyclized in solution to give the poly(ester-imide) *m*-**8d**. A mixture of 2 mL of pyridine and 5 mL of acetic anhydride was added into the preceding poly(amic acid) solution, and the reaction mixture was stirred at room temperature for 2 h and then heated at 100 °C for 1 h. The resultant poly(ester-imide) solution was poured into 200 mL of methanol to give a light yellow precipitate which was collected by filtration, washed thoroughly with methanol and hot water and then dried at 100 °C in a vacuum oven. The yield was almost quantitative. The FT-IR spectrum (thin-film) exhibited characteristic absorptions at 1,778 $cm^{-1}$ (imide asymmetrical C=O stretching), 1,724–1,734 $cm^{-1}$ (imide symmetrical and ester C=O stretching), 1,375 $cm^{-1}$ (C–N stretching), 1,244, 1,116 $cm^{-1}$ (asymmetrical and symmetrical C–O–C stretching), and 725 $cm^{-1}$ (imide ring deformation). All of other poly(ester-imide)s were synthesized by using a similar procedure as above.

## Preparation of the polymer films

For the ‘organosoluble’ poly(ester-amide)s and poly (ester-imide)s, the samples were cast into films by using the solvent-casting technique. A polymer solution was made by dissolving about 0.5 g of the polymer sample in 5 mL of DMAc to afford an approximately 10 wt% solution. After the polymer was completely dissolved, the homogeneous solution was poured into a 7 cm diameter glass Petri dish and then placed in a oven overnight (at 90 °C) to enable slow evaporation of the cast solvent. The ‘semi-dried’ polymer film was stripped off from the glass substrate and further dried *in vacuo* at 160 °C for 8 h. The obtained films, about 0.1 mm in

thickness, were used for X-ray diffraction measurements, tensile tests, solubility tests and thermal analysis.

## Measurements

Elemental analysis was carried out on a Heraeus VarioEL-III C, H, N analyzer. Infrared spectra were recorded on a Horiba FT-720 Fourier-transform infrared (FT-IR) spectrometer. $^{1}H$ and $^{13}C$ NMR spectra were measured on a JEOL EX-400 NMR spectrometer with perdeuterodimethyl sulfoxide (DMSO-$d_6$) as the solvent and tetramethylsilane as the internal reference, operating at 400 and 100 MHz, respectively. The inherent viscosities of the poly(ester-amide)s were obtained at a concentration of 0.5 g/dL in DMAc containing 5 wt% LiCl using a Cannon-Fenske viscometer at 30 °C. The inherent viscosities of the poly (ester-imide)s were measured at a concentration of 0.5 g/dL in DMAc with an Ubbelohde viscometer at 30 °C. Gel permeation chromatography (GPC) was carried out on a Waters chromatography unit interfaced with a Waters 2410 refractive-index detector. Two Waters 5 μm columns, Styragel HR-2 and HR-4 (7.8 mm inside diameter× 300 mm), connected in series, were used with tetrahydrofuran (THF) as the eluent and were calibrated with narrow-polydispersity polystyrene standards. Wide-angle X-ray diffraction (WAXD) measurements were performed at room temperature (about 25 °C) on a Shimadzu XRD 6000 X-ray diffractometer (40 kV, 20 mA), using graphite-monochromatized Cu-Kα radiation. An Instron universal tester (Model 4400R) with a load cell of 5 kg was used to study the stress–strain behavior of the polymer film samples. A gauge length of 2 cm and a crosshead speed of 5 mm/min were employed in this study. Measurements were performed at room temperature with film specimens (0.5 cm wide, 6 cm long and about 0.1 mm thick), and an average of at least three replicas was used. Thermogravimetric analysis (TGA) was conducted with a Perkin-Elmer Pyris 1 TGA instrument. These experiments were carried out on approximately 6–8 mg film or powder samples heated under flowing nitrogen or air (40 mL/min), at a heating rate of 20 °C/min from 200 to 800 °C. Differential scanning calorimetry (DSC) analysis was performed on a Perkin-Elmer Pyris 1 DSC instrument, at a scanning rate of 20 °C/min from 50 to 400 °C under flowing nitrogen (20 mL/min). The glass-transition temperatures ($T_g$s) were read at the midpoint of the transition in the heat capacity and were taken from the second heating trace after rapid cooling from 400 °C at a cooling rate of 200 °C/min. Thermomechanical analysis

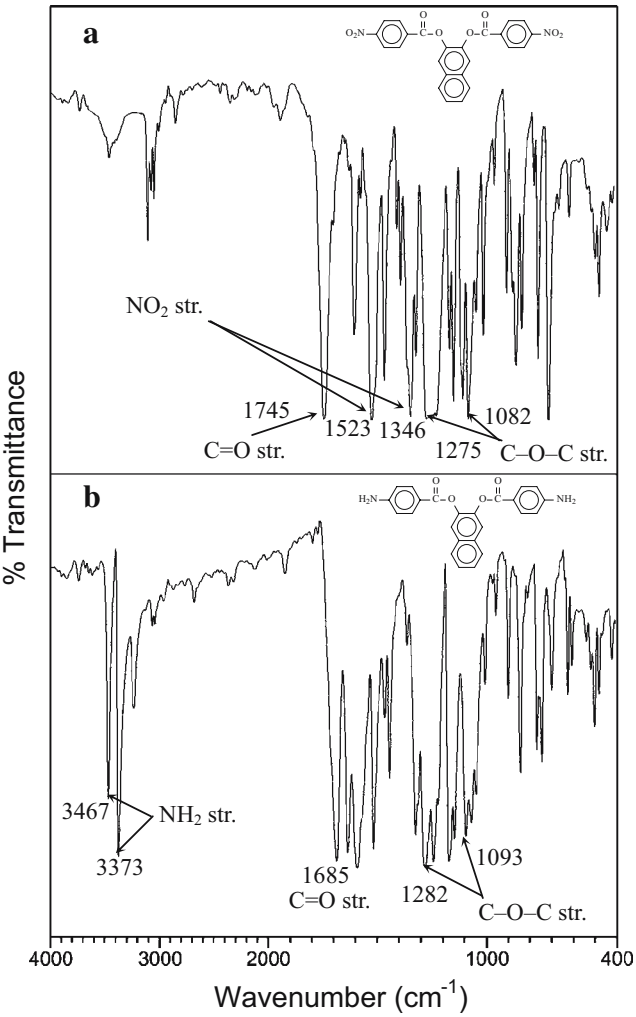


**Fig. 1** FT-IR spectra of **a** the dinitro-diester *p*-**1** and **b** the bis(ester-amine) *p*-**2**

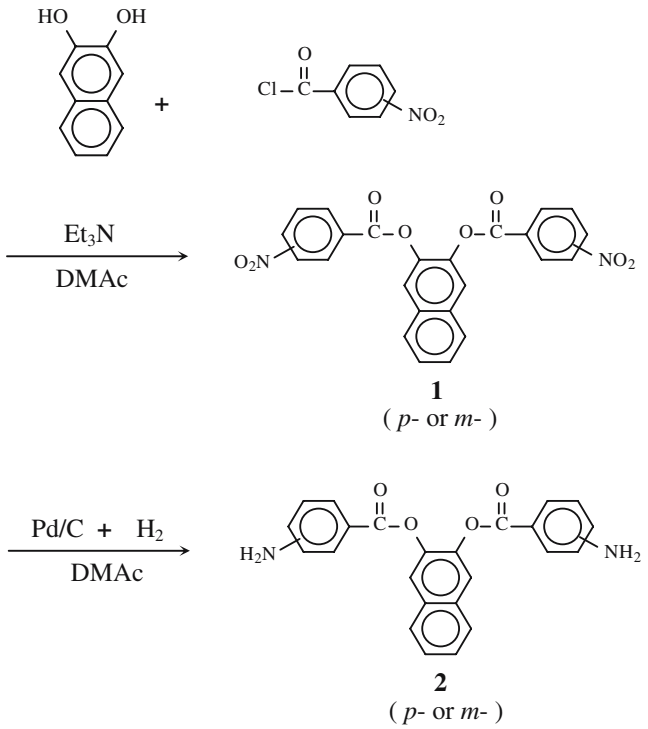


**Scheme 1** Synthetic route used to prepare the bis(ester-amine) *p*-**2** and *m*-**2**

(TMA) was carried out on a Perkin-Elmer TMA 7 instrument. The TMA experiments were conducted from 50 to 300 °C at a heating rate of 10 °C/min using a penetration probe of 1.0 mm in diameter under an applied constant load of 10 mN. The softening temperatures ($T_s$) were taken as the onset temperatures of the probe displacement on the TMA traces.

## Results and discussion

### Synthesis of bis(ester-amine)s

The new bis(ester-amine)s *p*-**2** and *m*-**2** were successfully synthesized by using the hydrogen Pd/C-catalysed reduction of the dinitro-diester compounds *p*-**1** and *m*-**1** resulting from the condensation reaction of 2,3-dihydroxynaphthalene with 4-nitrobenzoyl chloride and 3-nitrobenzoyl chloride, respectively, as shown in Scheme 1. Elemental analysis, plus IR and NMR spectroscopy were used to confirm the structures of all intermediates and monomers. The elemental analysis values were generally in agreement with the calculated values for the proposed structures. The FT-IR spectra of the *p*-**1** and *p*-**2** and the *m*-**1** and *m*-**2** are illustrated in Figs. 1 and 2, respectively. The nitro groups of the *p*-**1** showed two characteristic absorption bands at 1,523 (asymmetrical $NO_2$ stretching) and 1,346 (symmetrical $NO_2$ stretching) $cm^{-1}$. After the reduction, the characteristic absorptions of the nitro groups disappeared, and the amino groups showed a pair of N–H stretching absorption bands at 3,467 (asymmetrical $NH_2$ stretching) and 3,373 (symmetrical $NH_2$ stretching) $cm^{-1}$. In the FT-IR spectrum of bis (ester-amine) *p*-**2**, the characteristic absorption band at 1,685 $cm^{-1}$ was assigned to the ester carbonyl group, which was about 60 $cm^{-1}$ lower than that of the dinitro-diester *p*-**1** (1,745 $cm^{-1}$). Conjugation of the amino group substituted at the *para*-position caused the absorption shift. The structures of the bis(ester-amine)s *p*-**2** and *m*-**2** were also

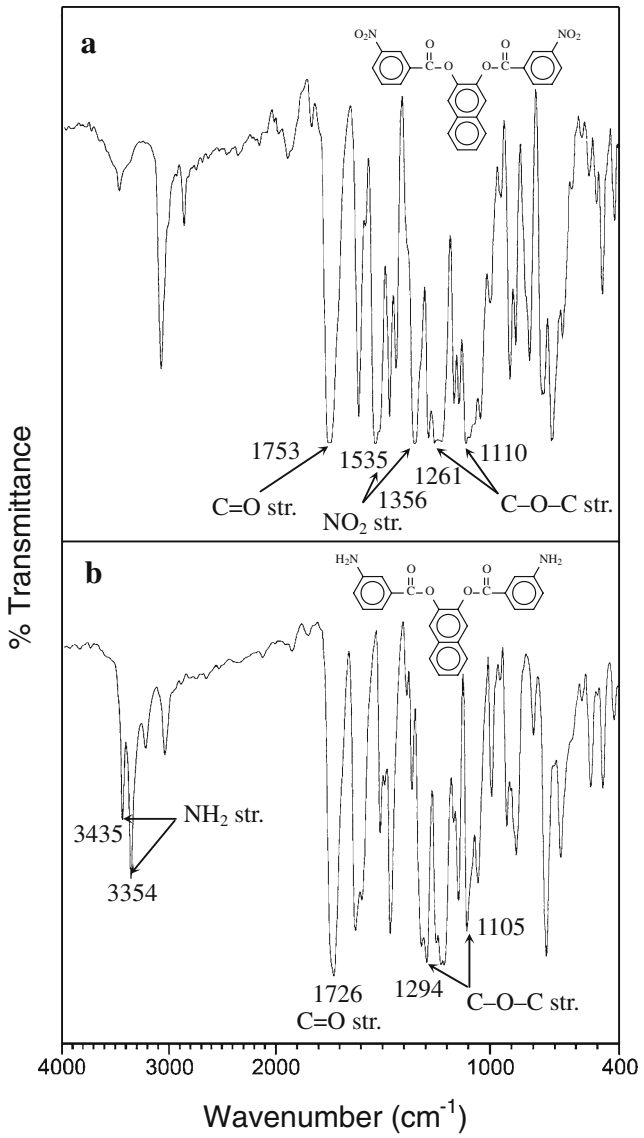


**Fig. 2** FT-IR spectra of **a** the dinitro-diester *m*-**1** and **b** the bis(ester–amine) *m*-**2**

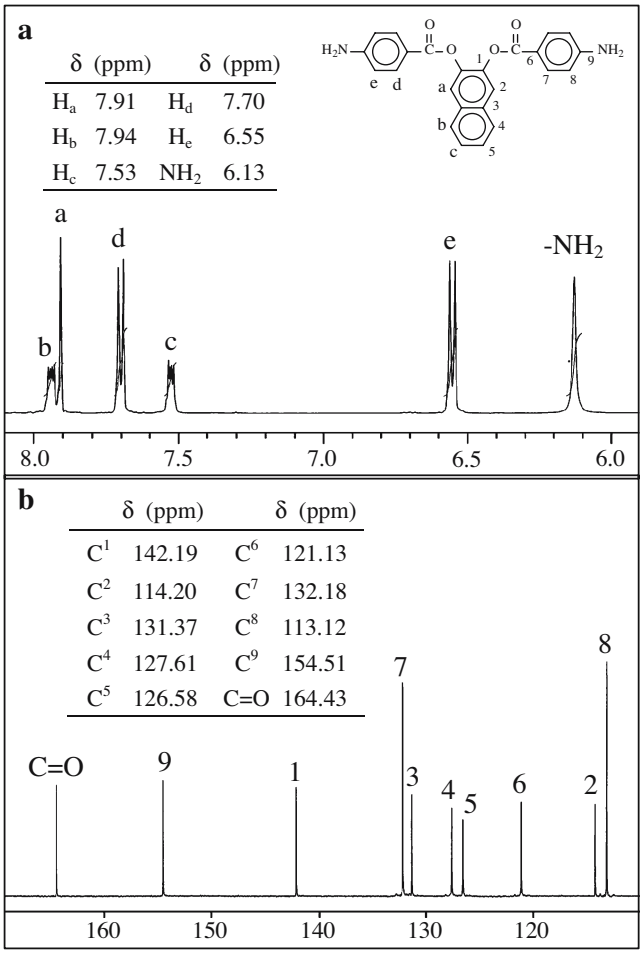


**Fig. 3** **a** $^1$H NMR and **b** $^{13}$C NMR spectra of the bis(ester–amine) *p*-**2** in DMSO-$d_6$

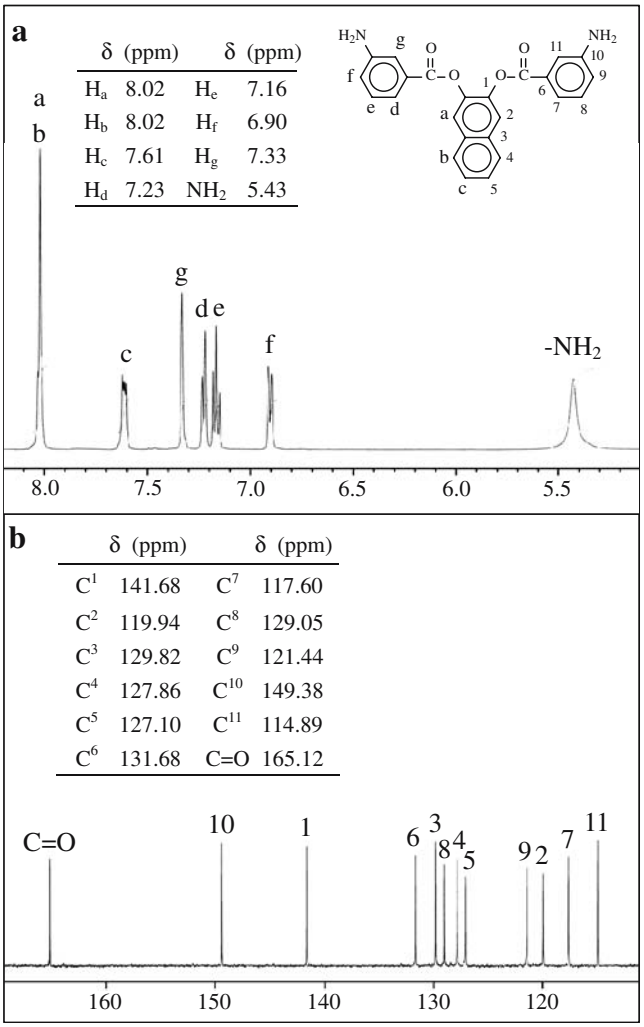


**Fig. 4** **a** $^{1}$H NMR and **b** $^{13}$C NMR spectra of the bis(ester–amine) *m*-**2** in DMSO-$d_6$

identified by high-resolution NMR spectroscopy. The $^{1}$H NMR and $^{13}$C NMR spectra of the bis(ester-amine)s *p*-**2** and *m*-**2** are shown in Figs. 3 and 4, respectively. The assignments of each carbon and proton are also given in the figures, and all the NMR spectroscopic data are consistent with the proposed molecular structures. In the $^{1}$H-NMR spectra, a downfield chemical shift ($\delta_H$ is increased) usually corresponds to the decrease in the electron-donating property of the amino group. The electron-withdrawing effect is stronger for the *para*-substituted ester carbonyl group than that substituted at the *meta*-position. Thus, the nucleophilicity for the amino groups of bis(ester-amine) *m*-**2** ($\delta_H$=5.43 ppm) was expected to be stronger than those of its *para*-isomer ( *p*-**2**; $\delta_H$=6.13 ppm). It also can be seen from the $^{13}$C NMR spectra that the amino group attached carbon atoms ($C^9$) in *p*-**2** resonated at a lower field ($\delta$= 154.51 ppm) compared to the corresponding ones ($C^{10}$) in *m*-**2** ($\delta$=149.38 ppm) because of the stronger electron-withdrawing effect of the carbonyl group in the former.

Synthesis of poly(ester-amide)s

The direct polycondensation of aromatic diamines with aromatic dicarboxylic acids in NMP solution containing dissolved $CaCl_2$ using triphenyl phosphite (TPP) and pyridine as condensing agents is known to be a convenient method for the preparation of aromatic polyamides on the laboratory scale [48]. This method was adopted here to prepare two series of aromatic homopoly(ester-amide)s *p*-**5a-e** and *m*-**5a-e** from the bis(ester-amine)s *p*-**2** and *m*-**2**, respectively, with various aromatic dicarboxylic acids **4a-e**, as shown in Scheme 2. Two series of random copoly (ester-amide)s *p*-**5f-j** and *m*-**5f-j** were also prepared from an equimolar mixture of the bis(ester-amine)s and 4,4′-oxydianiline with various aromatic dicarboxylic acids **4a-e**. The inherent viscosities of poly(ester-amide)s *p*-**5a-j** and *m*-**5a-j** are summarized in Table 1. These two series of poly (ester-amide)s were obtained in almost quantitative yields with inherent viscosities of 0.32–0.65 dL/g for *p*-**5a-j** and 0.38–0.68 dL/g for *m*-**5a-j**. As can be seen from Table 2, the GPC data obtained for *p*-**5b**, *p*-**5d**, *p*-**5 i**, *m*-**5b-e**, and *m*-**5i** indicated that the *M*w and *M*n values were in the range 13,400–30,300 and 9,500–15,000 g/mol, respectively, on the basis of polystyrene standards. Except for *p*-**5a** and *p*-**5f**, all the other poly(ester-amide)s could be solution-cast into free-

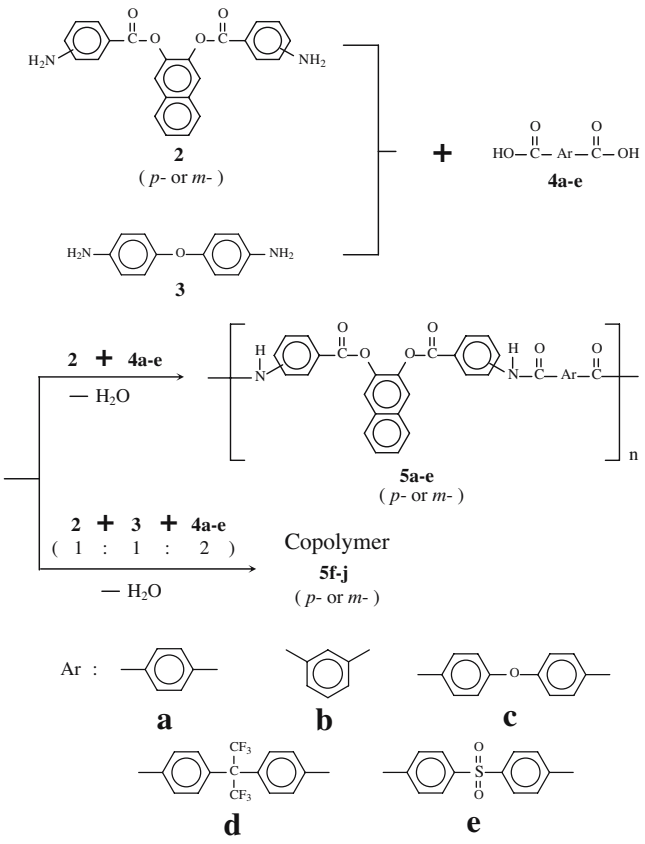


**Scheme 2** Synthesis of poly(ester-amide)s

**Table 1** Inherent viscosities, film quality, and tensile properties of the poly(ester-amide)s and poly(ester-imide)s

| Polymer | $\eta_{inh}$[a] (dL/g) | Film quality[b] | Tensile properties of films | | |
|---|---|---|---|---|---|
| | | | Tensile strength (MPa) | Elongation to break (%) | Initial modulus (GPa) |
| *p*-**5a** | 0.32 | –[c] | –[d] | – | – |
| *p*-**5b** | 0.48 | B | – | – | – |
| *p*-**5c** | 0.56 | B | – | – | – |
| *p*-**5d** | 0.48 | B | – | – | – |
| *p*-**5e** | 0.45 | B | – | – | – |
| *p*-**5f** | 0.38 | – | – | – | – |
| *p*-**5g** | 0.58 | F | 82 | 7 | 1.7 |
| *p*-**5h** | 0.65 | F | 85 | 10 | 1.8 |
| *p*-**5i** | 0.54 | F | 79 | 8 | 1.8 |
| *p*-**5j** | 0.58 | F | 84 | 11 | 2.1 |
| *m*-**5a** | 0.38 | B | – | – | – |
| *m*-**5b** | 0.45 | B | – | – | – |
| *m*-**5c** | 0.51 | B | – | – | – |
| *m*-**5d** | 0.47 | B | – | – | – |
| *m*-**5e** | 0.47 | B | – | – | – |
| *m*-**5f** | 0.45 | B | – | – | – |
| *m*-**5g** | 0.52 | B | – | – | – |
| *m*-**5h** | 0.58 | B | – | – | – |
| *m*-**5i** | 0.52 | F | 75 | 8 | 1.8 |
| *m*-**5j** | 0.68 | F | 81 | 10 | 2.0 |
| *p*-**8a** | −(0.34)[e] | – | – | – | – |
| *p*-**8b** | 0.29 (0.36) | B | – | – | – |
| *p*-**8c** | −(0.37) | – | – | – | – |
| *p*-**8d** | 0.45 (0.58) | F | 91 | 7 | 2.2 |
| *m*-**8a** | −(0.28) | – | – | – | – |
| *m*-**8b** | 0.25 (0.33) | B | – | – | – |
| *m*-**8c** | −(0.49) | – | – | – | – |
| *m*-**8d** | 0.48 (0.65) | F | 89 | 8 | 2.0 |

[a] Measured at a concentration of 0.5 g/dL in DMAc containing 5 wt% LiCl at 30 °C for the poly(ester-amide)s and at a concentration of 0.5g/dL in DMAc at 30 °C for the poly(ester-imide)s

[b] Films were cast by slow evaporation of polymer solutions in DMAc: *F* Flexible, *B* brittle.

[c] Insoluble in available organic solvents

[d] No available samples

[e] Inherent viscosities of the poly(amic acid) precursors measured at a concentration of 0.5 g/dL in DMAc at 30 °C

standing films. Some of the poly(ester-amide)s such as *p*-**5g-j** and *m*-**5i-j** could be cast into transparent, flexible, and strong films from DMAc solutions, indicative of the formation of high-molecular-weight polymers. However, the other films cracked upon creasing, possibly because of a higher level of crystallinity or lower molecular weight.

The structural features of the poly(ester-amide)s were verified by FT-IR spectroscopy and elemental analysis. A typical FT-IR spectrum of polymer *m*-**5j** is illustrated in Fig. 5. They showed the characteristic IR absorptions of the amide group at around 3,310–3,340 $cm^{-1}$ (N–H stretching), 1,660–1,680 $cm^{-1}$ (amide C=O stretching) and 1,500–1,530 $cm^{-1}$ (N–H bending). All of the poly(ester-amide)s also exhibited strong characteristic absorption bands at around 1,730–1,750 $cm^{-1}$ (ester C=O stretching), and at 1,240–1,270 $cm^{-1}$ and 1,080–1,100 $cm^{-1}$ (asymmetrical and symmetrical C–O–C stretching, respectively) due to the ester groups. The results of the elemental analysis of all of the homopoly(ester-amide)s are reported in Table 3. These data are in good agreement with the proposed structures, with the exception of the % C values, which are always lower than the theoretical ones. This can possibly be attributed to the very aromatic nature of these polymers, which commonly leave a small coal residue during the standard conditions of microanlysis. Another possible reason may be due to the hygroscopic nature of the amide groups of these polymers.

**Table 2** Average molecular weights of the poly(ester-amide)s and poly(ester-imide)s

| Polymer | $M_n$[a] | $M_w$[a] | $M_w/M_n$ |
|---|---|---|---|
| *p*-**5b** | 10,500 | 17,600 | 1.68 |
| *p*-**5d** | 11,800 | 21,900 | 1.86 |
| *p*-**5i** | 15,000 | 30,300 | 2.02 |
| *m*-**5b** | 9,500 | 13,600 | 1.43 |
| *m*-**5c** | 12,700 | 25,600 | 2.02 |
| *m*-**5d** | 10,900 | 18,700 | 1.72 |
| *m*-**5e** | 9,800 | 13,400 | 1.37 |
| *m*-**5i** | 13,500 | 21,900 | 1.62 |
| *p*-**8d** | 10,300 | 13,700 | 1.33 |
| *m*-**8b** | 7,100 | 8,700 | 1.23 |
| *m*-**8d** | 12,200 | 17,400 | 1.43 |

[a] Relative to polystyrene standards, using THF as the eluent

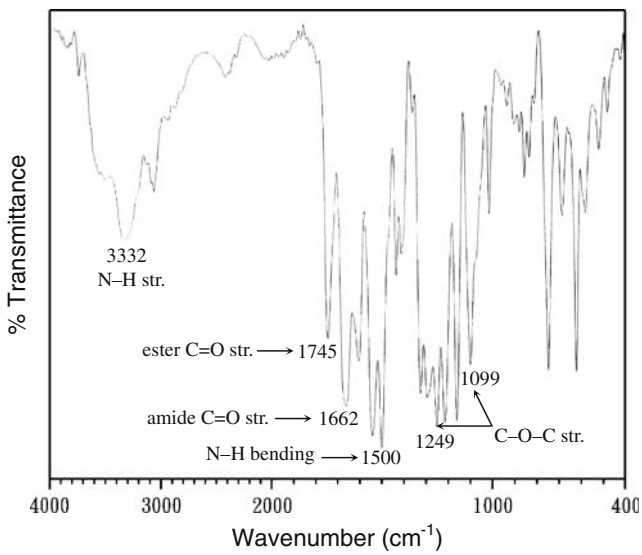


**Fig. 5** FT-IR spectrum of a thin film of the copoly(ester-amide) *m*-**5j**

**Table 3** Elemental analysis data for the poly(ester-amide)s and poly(ester-imide)s

| Polymer | Formula of the repeat unit (Formula weight) | C (%) | | H (%) | | N (%) | |
|---|---|---|---|---|---|---|---|
| | | Calculated | Found | Calculated | Found | Calculated | Found |
| *p*-**5a** | $C_{32}H_{20}N_2O_6$(528.52) | 72.72 | 71.79 | 3.81 | 3.91 | 5.30 | 5.21 |
| *p*-**5b** | $C_{32}H_{20}N_2O_6$(528.52) | 72.72 | 71.68 | 3.81 | 3.93 | 5.30 | 5.24 |
| *p*-**5c** | $C_{38}H_{24}N_2O_7$(620.62) | 73.54 | 72.85 | 3.90 | 4.02 | 4.51 | 4.39 |
| *p*-**5d** | $C_{41}H_{24}F_6N_2O_6$(754.64) | 65.26 | 64.57 | 3.21 | 3.32 | 3.71 | 3.63 |
| *p*-**5e** | $C_{38}H_{24}N_2O_8S$(668.68) | 68.26 | 67.19 | 3.62 | 3.74 | 4.19 | 4.07 |
| *m*-**5a** | $C_{32}H_{20}N_2O_6$(528.52) | 72.72 | 71.82 | 3.81 | 3.96 | 5.30 | 5.19 |
| *m*-**5b** | $C_{32}H_{20}N_2O_6$(528.52) | 72.72 | 71.64 | 3.81 | 3.95 | 5.30 | 5.22 |
| *m*-**5c** | $C_{38}H_{24}N_2O_7$(620.62) | 73.54 | 72.59 | 3.90 | 4.05 | 4.51 | 4.41 |
| *m*-**5d** | $C_{41}H_{24}F_6N_2O_6$(754.64) | 65.26 | 64.37 | 3.21 | 3.36 | 3.71 | 3.63 |
| *m*-**5e** | $C_{38}H_{24}N_2O_8S$(668.68) | 68.26 | 67.18 | 3.62 | 3.71 | 4.19 | 4.10 |
| *p*-**8a** | $C_{34}H_{16}N_2O_8$(580.51) | 70.35 | 69.37 | 2.78 | 2.82 | 4.83 | 4.85 |
| *p*-**8b** | $C_{43}H_{20}F_6N_2O_8$(806.63) | 64.03 | 63.42 | 2.50 | 2.54 | 3.47 | 3.55 |
| *m*-**8a** | $C_{34}H_{16}N_2O_8$(580.51) | 70.35 | 69.29 | 2.78 | 2.83 | 4.83 | 4.86 |
| *m*-**8b** | $C_{43}H_{20}F_6N_2O_8$(806.63) | 64.03 | 63.45 | 2.50 | 2.56 | 3.47 | 3.52 |

## Synthesis of poly(ester-imide)s

Four homopoly(ester-imide)s *p*-**8a,b** and *m*-**8a,b** were prepared from the bis(ester-amine)s *p*-**2** and *m*-**2**, respectively, with PMDA (**6a**) and 6FDA (**6b**) by the conventional two-stage synthetic method involving a ring-opening polyaddition and subsequent chemical cyclodehydration, as shown in Scheme 3. Four random copoly(ester-imide)s *p*-**8c,d** and *m*-**8c,d** were also prepared from an equimolar mixture of the bis(ester-amine)s and 4,4′-oxydianiline with dianhydrides PMDA and 6FDA. As shown in Table 1, the inherent viscosities of the intermediate poly(amic acid)s were in the range of 0.34–0.58 dL/g for *p*-**8a-d** and 0.28-0.65 dL/g for *m*-**8a-d** in DMAc. We had tried thermal cyclodehydration of the poly(amic acid)s; however, highly brittle polyimide films were usually obtained. It may be suggested that the ester linkages in the polymer chain may be hydrolyzed during imidization at elevated temperatures. Therefore, the precursor poly(amic acid)s obtained were chemically cyclized in solution to give the poly(ester-imide)s. The inherent viscosities of the organosoluble poly(ester-imide)s were recorded in 0.29–0.45 dL/g for *p*-**8b** and *p*-**8d** and 0.25–0.48 dL/g for *m*-**8b** and *m*-**8d**, as measured in DMAc at 30 °C. As shown in Table 2, the GPC data obtained for *p*-**8d**, *m*-**8b**, and *m*-**8d** indicated that the *M*w and *M*n values were in the range 8,700–17,400 and 7,100–12,200 g/mol, respectively, on the basis of polystyrene standards. The poly(ester-imide)s *p*-**8d** and *m*-**8d** could be solution-cast into transparent, flexible, and strong films, indicative of the formation of high-molecular-weight polymers. However, the poly(ester-imide)s *p*-**8b** and *m*-**8b** cracked upon creasing. The other poly(ester-imide)s *p*-**8a**, *p*-**8c**, *m*-**8a**, and *m*-**8c** derived from PMDA precipitated during chemical imidization and were insoluble in available organic solvents, possibly because of a high level of crystallinity or the structural rigidity of the pyromellitimide segment. Therefore, no attempts have been made to cast films from these insoluble polymers.

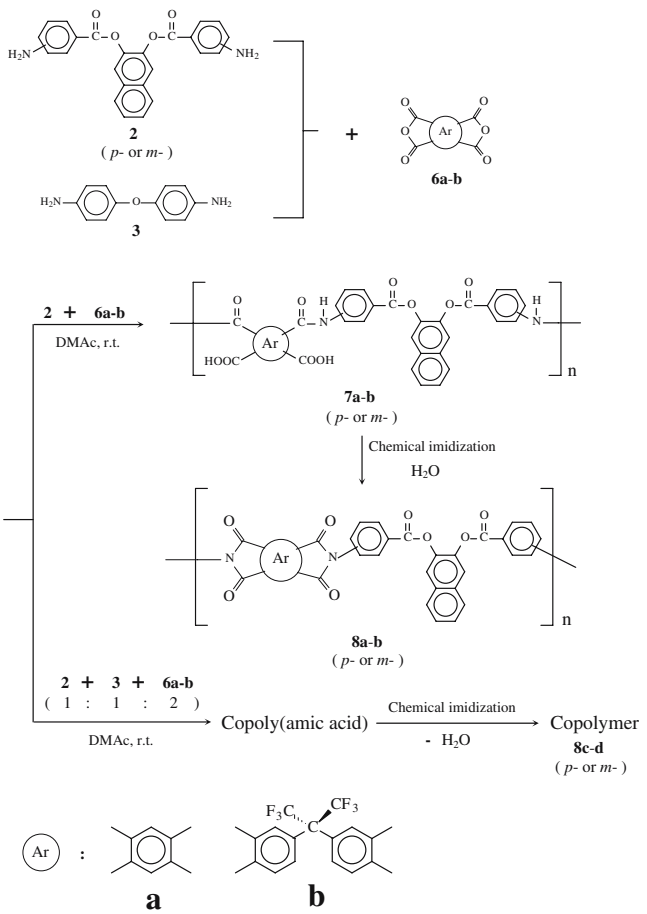


**Scheme 3** Synthetic route used to prepare the poly(ester-imide)s

The structural features of the poly(ester-imide)s were verified by FT-IR spectroscopy and elemental analysis. A typical set of FT-IR spectra for the poly(amic acid) *m*-**7d** and poly(ester-imide) *m*-**8d** is shown in Fig. 6. As it can be

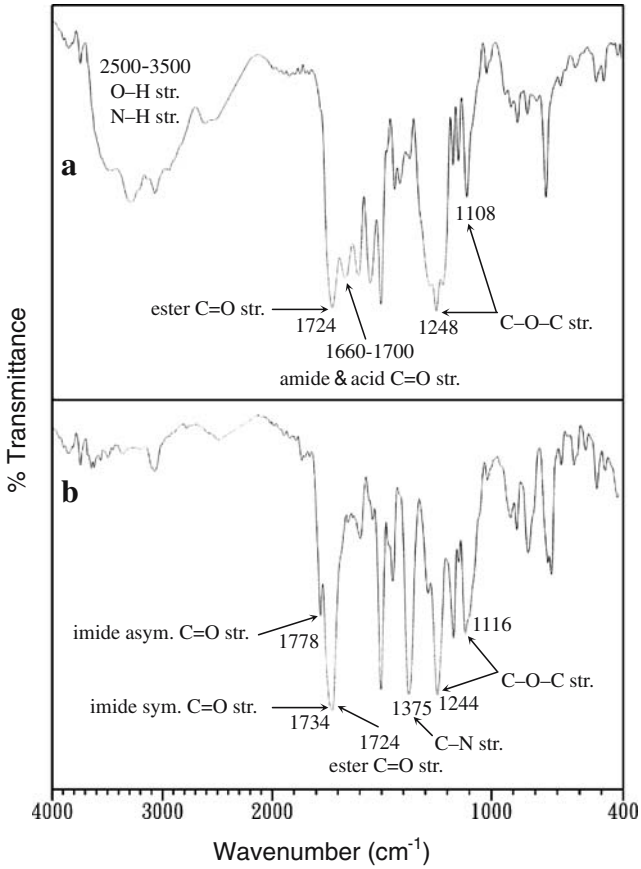


**Fig. 6** FT-IR spectra of **a** the poly(amic acid) precursor *m*-**7d** and **b** the poly(ester-imide) *m*-**8d**

seen, the spectra are in good agreement with the proposed structures. All of the poly(amic acid)s revealed characteristic absorption bands at around 1,660–1,700 $cm^{-1}$ (amide and acid C=O stretching) and 2,500–3,500 $cm^{-1}$ (O–H and N–H stretching). The disappearance of the amic acid bands indicates a virtually complete conversion of the poly(amic acid) precursor into the polyimide. The characteristic absorption bands of the imide rings appeared at around 1,778 and 1,734 $cm^{-1}$ (typical of imide carbonyl asymmetrical and symmetrical stretching), 1,375 $cm^{-1}$ (C–N stretching), and 720 $cm^{-1}$ (imide ring deformation). All of the poly (amic acid)s and poly(ester-imide)s also exhibited strong characteristic absorption bands at around 1,720–1,740 $cm^{-1}$ (ester C=O stretching) and 1,240–1,270, 1,080–1,120 $cm^{-1}$ (asymmetrical and symmetrical C–O–C stretching) due to the ester groups. The results of the elemental analysis of all of the homopoly(ester-imide)s are also compiled in Table 3. The elemental analysis values were generally in good agreement with the calculated values for the proposed formulas.

## Properties of poly(ester-amide)s

All of the poly(ester-amide)s were characterized by WAXD studies. The diffractograms shown in Fig. 7 indicate that all of the poly(ester-amide)s, except polymers *p*-**5a** and *p*-**5f**, are amorphous. The homopoly(ester-amide) *p*-**5a** and copoly(ester-amide) *p*-**5f** derived from the more rigid and symmetrical terephthalic acid (**4a**) and the *para*-linked bis (ester-amine) *p*-**2** displayed some strong diffraction signals assignable to a semicrystalline nature and did not afford ductile films. The copoly(ester-amide)s *p*-**5g-j** and *m*-**5i-j** that could afford flexible and tough films (as listed in Table 1) showed amorphous patterns. The other homopoly (ester-amide)s and copoly(ester-amide)s which could afford free-standing films but cracked upon creasing also revealed amorphous patterns.

The solubility of these poly(ester-amide)s was tested qualitatively in various organic solvents, and the results are reported in Table 4. In general, the semicrystalline polymers displayed a low solubility. For example, *p*-**5a** and *p*-**5f** were insoluble in any of the solvents tested. In contrast, the

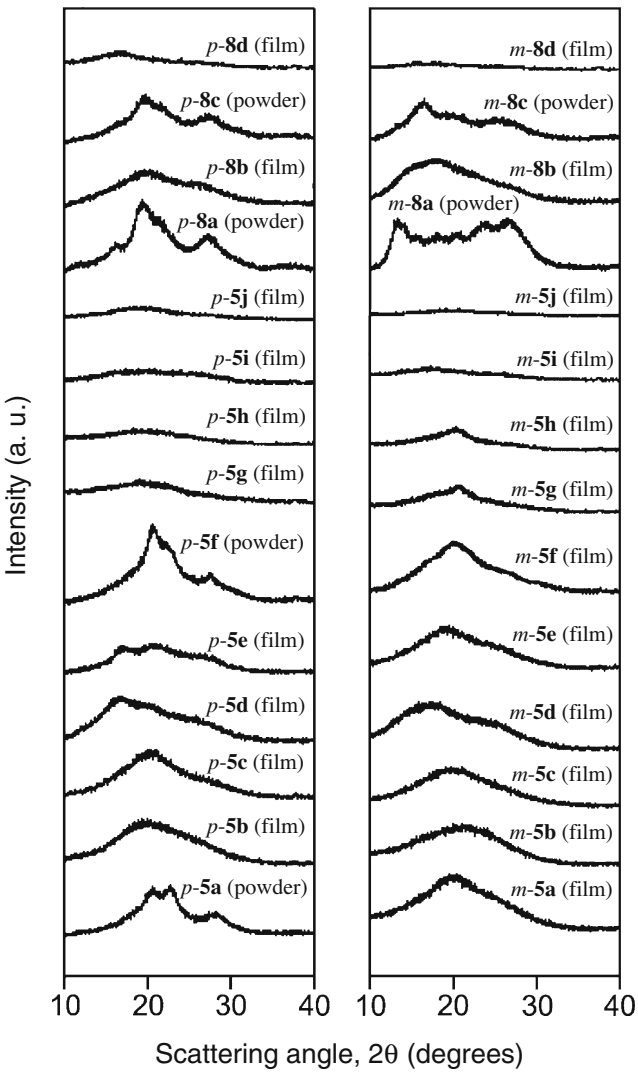


**Fig. 7** WAXD patterns of the poly(ester-amide)s and poly(ester-imide)s

**Table 4** Solubility behaviour of the poly(ester-amide)s and poly (ester-imide)s

| Polymer | Solubility[a] | | | | | |
|---|---|---|---|---|---|---|
| | NMP | DMAc | DMF | DMSO | *m*-Cresol | THF |
| *p*-**5a** | − | − | − | − | − | − |
| *p*-**5b** | + | + | + | + | + | + |
| *p*-**5c** | + | + | + | + | + | − |
| *p*-**5d** | + | + | + | + | + | + |
| *p*-**5e** | + | + | + | + | − | − |
| *p*-**5f** | − | − | − | − | − | − |
| *p*-**5g** | + | + | + | + | + | − |
| *p*-**5h** | + | + | + | + | − | − |
| *p*-**5i** | + | + | + | + | + | + |
| *p*-**5j** | + | + | + | + | + | − |
| *m*-**5a** | + | + | + | + | + | − |
| *m*-**5b** | + | + | + | + | + | + |
| *m*-**5c** | + | + | + | + | + | + |
| *m*-**5d** | + | + | + | + | + | + |
| *m*-**5e** | + | + | + | + | + | + |
| *m*-**5f** | + | + | + | + | − | − |
| *m*-**5g** | + | + | + | + | + | − |
| *m*-**5h** | + | + | + | + | − | − |
| *m*-**5i** | + | + | + | + | + | + |
| *m*-**5j** | + | + | + | + | + | − |
| *p*-**8a** | − | − | − | − | − | − |
| *p*-**8b** | + | + | + | − | + | − |
| *p*-**8c** | − | − | − | − | − | − |
| *p*-**8d** | + | + | + | − | + | + |
| *m*-**8a** | − | − | − | − | − | − |
| *m*-**8b** | + | + | + | + | + | + |
| *m*-**8c** | − | − | − | − | − | − |
| *m*-**8d** | + | + | + | + | + | + |

[a] Qualitative solubility tested with 10 mg of sample in 1 mL of the solvent: + Soluble at room temperature, − insoluble even on heating, *NMP N*-methyl-2-pyrrolidone, *DMAc N,N*-dimethylacetamide, *DMF N, N*-dimethylformamide, *DMSO* dimethyl sulfoxide, *THF* tetrahydrofuran

amorphous nature of the other polymers was reflected in their excellent solubility. The amorphous poly(ester-amide)s *p*-**5b-e**, *p*-**5g-j**, and *m*-**5a-j** exhibited a higher solubility; they were readily soluble in highly polar solvents, such as NMP, DMAc, DMF, and DMSO at room temperature. Some of them were even soluble in less polar *m*-cresol and THF at room temperature. Thus, such excellent solubility makes these polymers potential candidates for practical applications in spin-on and casting processes. As previously mentioned, the copoly(ester-amide)s *p*-**5g-j** and *m*-**5i-j** could be solution-cast into flexible and tough films. These thin films were of good quality, creasable and suitable for tensile testing, and their tensile properties are also presented in Table 1. These films exhibited ultimate tensile strengths to break of 75–85 MPa, elongations to break of 7–11%, and initial moduli of 1.7–2.1 GPa. They can be considered good for films made on a laboratory scale.

The thermal behavior data of the poly(ester-amide)s, evaluated by DSC, TMA and TGA, are summarized in Table 5. In the DSC experiments, the poly(ester-amide)s *p*-**5a** and *p*-**5f** showed a clear medium-intensity melting endotherm with a peak temperature at 346 and 381 °C, respectively, and no discernible $T_g$s were observed on the heating DSC curves probably because of their semicrystalline nature. These results correspond to their WAXD patterns shown in Fig. 7. Most of the poly(ester-amide)s showed clear $T_g$ values between 192 and 223 °C by DSC. A typical DSC thermogram for the representative poly(ester-amide) *p*-**5i** is illustrated in Fig. 8. None of the polymers, except *p*-**5a** and *p*-**5f**, showed a clear melting endotherm in their DSC heating traces. This supports the amorphous nature of these poly(ester-amide)s. The *p*-**5** series poly(ester-amide)s generally showed a higher $T_g$ as compared with the corresponding *m*-**5** series counterparts because of the higher cohesive energies associated with the higher linearity imposed by the *para* catenation, instead of the *meta* catenation of the diamine moiety. The copoly(ester-amide)s *p*-**5f-j** and *m*-**5f-j** also showed a higher $T_g$ as compared with the corresponding homopoly(ester-amide)s *p*-**5a-e** and *m*-**5a-e** counterparts because of an enhanced chain rigidity of 4,4′-oxydianiline as compared to the bis(ester-amine)s. The poly(ester-amide) *m*-**5f** exhibited the highest $T_g$ value (223 °C) probably due to the more rigid and symmetrical diacid residue derived from terephthalic acid (**4a**). The softening temperature ($T_s$) values of the tough poly(ester-amide) films, measured by TMA, were recorded in the range 202–218 °C. A typical TMA thermogram of polymer *p*-**5i** is also illustrated in Fig. 8. In most cases, the $T_s$ values obtained by TMA are comparable to the $T_g$ values measured by the DSC experiments. The trend in variation of $T_s$ is similar to that of the $T_g$ observed in the DSC measurements. Probably due to the presence of flexible ester linkages, the poly(ester-amide)s generally exhibited lower $T_g$ values in comparison with the corresponding poly (ether-amide)s reported in literature [37].

The thermal and thermo-oxidative stabilities of these poly(ester-amide)s were evaluated by TGA under both nitrogen and air atmospheres using the 5 and 10 wt% loss temperatures ($T_d$) for comparison (Table 5). The amounts of carbonized residues (char yields) at 800 °C in nitrogen for these poly(ester-amide)s were in the range 50–66 wt%. The $T_d$ values at 5 wt% loss for all of the poly(ester-amide)s were recorded in the range 303–421 °C in nitrogen and in the range 299–420 °C in air, which were lower than those of the analogous poly(ether-amide)s [37] because of the less stable ester groups. A comparison of the TGA behaviour in nitrogen and air atmospheres for the representative poly (ester-amide) *p*-**5j** is shown in Fig. 9. This polymer showed very similar TGA behaviour in nitrogen and air atmospheres below 500 °C, but when the temperature was

**Table 5** Thermal properties of the poly(ester-amide)s and poly(ester-imide)s

| Polymer | $T_g$ (°C)[a] | $T_s$ (°C)[b] | $T_d$ at 5 wt% loss (°C)[c] | | $T_d$ at 10 wt% loss (°C)[c] | | Char yield (%)[d] |
|---|---|---|---|---|---|---|---|
| | | | In $N_2$ | In air | In $N_2$ | In air | |
| *p*-**5a** | –[e] (346)[f] | –[g] | 337 | 339 | 364 | 365 | 57 |
| *p*-**5b** | 216 | – | 303 | 299 | 329 | 325 | 52 |
| *p*-**5c** | – | – | 362 | 374 | 414 | 419 | 58 |
| *p*-**5d** | 199 | – | 338 | 344 | 369 | 383 | 50 |
| *p*-**5e** | – | – | 381 | 381 | 426 | 418 | 59 |
| *p*-**5f** | –(381) | – | 421 | 420 | 462 | 459 | 58 |
| *p*-**5g** | 219 | 217 | 374 | 390 | 413 | 430 | 58 |
| *p*-**5h** | 221 | 217 | 395 | 409 | 437 | 450 | 58 |
| *p*-**5i** | 211 | 214 | 379 | 389 | 429 | 432 | 55 |
| *p*-**5j** | 220 | 218 | 412 | 406 | 444 | 440 | 58 |
| *m*-**5a** | 219 | – | 350 | 356 | 381 | 389 | 62 |
| *m*-**5b** | 195 | – | 371 | 366 | 399 | 394 | 63 |
| *m*-**5c** | 201 | – | 393 | 401 | 433 | 433 | 62 |
| *m*-**5d** | 192 | – | 376 | 396 | 418 | 437 | 54 |
| *m*-**5e** | 202 | – | 339 | 346 | 376 | 383 | 59 |
| *m*-**5f** | 223 | – | 356 | 361 | 415 | 424 | 66 |
| *m*-**5g** | 210 | – | 405 | 408 | 436 | 441 | 61 |
| *m*-**5h** | 214 | – | 397 | 408 | 438 | 452 | 61 |
| *m*-**5i** | 204 | 202 | 390 | 408 | 440 | 456 | 57 |
| *m*-**5j** | 213 | 208 | 388 | 399 | 427 | 441 | 62 |
| *p*-**8a** | – | – | 492 | 492 | 527 | 525 | 49 |
| *p*-**8b** | 244 | – | 461 | 461 | 493 | 500 | 49 |
| *p*-**8c** | 265 | – | 467 | 453 | 524 | 516 | 54 |
| *p*-**8d** | 257 | 257 | 461 | 440 | 504 | 483 | 53 |
| *m*-**8a** | 245 | – | 467 | 455 | 496 | 487 | 50 |
| *m*-**8b** | 225 | – | 461 | 462 | 488 | 489 | 49 |
| *m*-**8c** | 252 | – | 481 | 488 | 515 | 534 | 55 |
| *m*-**8d** | 247 | 242 | 477 | 462 | 510 | 491 | 52 |

[a] Middle-point temperature of the baseline shift on the DSC heating trace (rate of 20 °C/min) from 50 to 400 °C after rapid cooling from 400 °C at a rate of 200 °C/min

[b] Softening temperature was measured by TMA (penetration method) with a constant applied load of 10 mN at a heating rate of 10 °C/min. The film samples were heated at 250 °C for 30 min before the TMA experiments.

[c] Decomposition temperature was recorded by TGA at a heating rate of 20 °C/min.

[d] Residual weight percent at 800 °C in $N_2$

[e] No discernible transition was observed.

[f] Peak-temperature of the medium-intensity melting endotherm on the first DSC heating trace (rate of 20 °C/min) from 50 to 400 °C.

[g] Not detected because of no available specimens

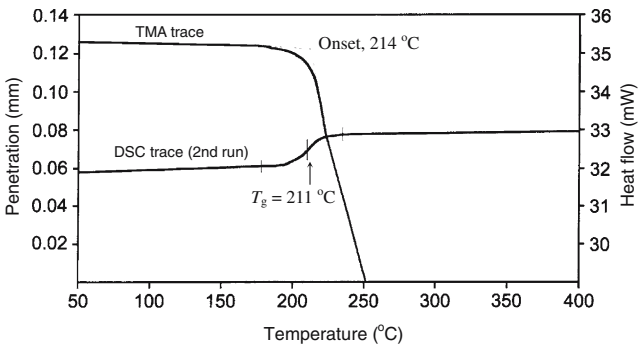


**Fig. 8** Typical DSC and TMA thermagrams of the poly(ester-amide) *p*-5i: DSC, heating rate of 20 °C/min; TMA, heating rate of 10 °C/min and applied force of 10 mN

increased above 500 °C, the polymer showed a rapid weight loss and decomposed almost completely at 700 °C in air. All of the poly(ester-amide)s seemed to exhibit a two-stage decomposition behaviour at elevated temperatures. The first stage of weight loss starting around 300 °C might be attributed to the early degradation of the less stable ester groups. The FT-IR spectra of the solid residues of the polymers after heat treatment were examined. Figure 10 shows FT-IR spectra of a thin film of the representative poly (ester-amide) *p*-**5h** after being heated sequentially in air, each for 10 min at 300, 350, 400 and 450 °C. The FT-IR spectra of *p*-**5h** after heat treatment at 300 and 350 °C remained almost the same as that before heat treatment. After heating

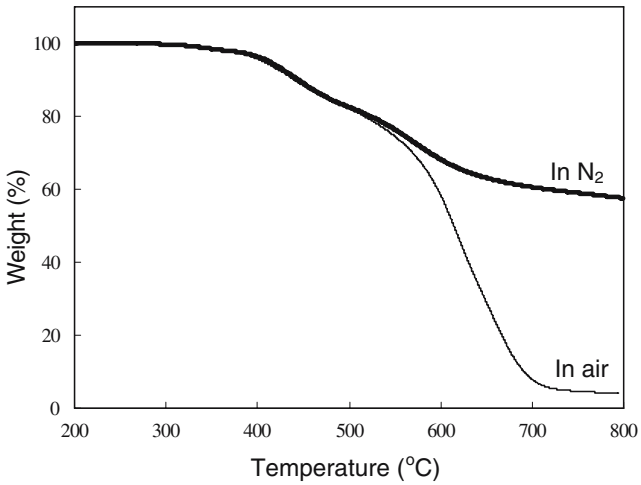


**Fig. 9** TGA curves of the poly(ester-amide) *p*-**5j** in nitrogen and air (heating rates of 20 °C/min)

at 400 °C for 10 min, an obvious decrease in the relative intensities at around 1,739, 1,265 and 1,068 $cm^{-1}$ indicated some loss of ester functionalities. After further heating at 450 °C for 10 min, the absorption bands of the ester groups almost completely disappeared, while a high content of amide functionalities and aromatic skeletons was still detected. The aforementioned results showed that these poly(ester-amide)s seemed to start to decompose from the weaker ester linkages.

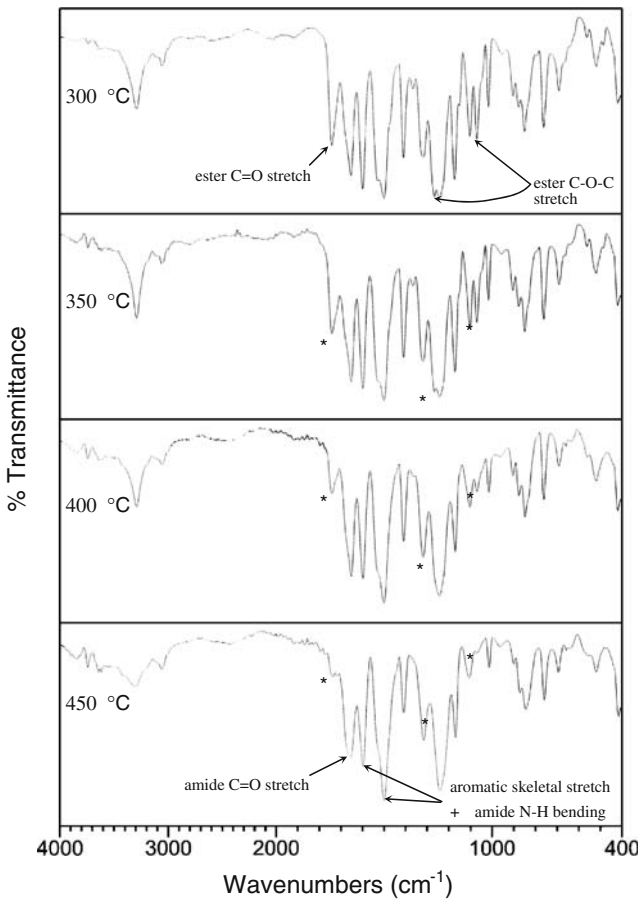


**Fig. 10** FT-IR spectra (thin-film sample) of the poly(ester-amide) *p*-**5h** after sequential heating in air at the indicated temperatures, each for 10 min (*asterisk* indicates the characteristic absorptions of the ester groups)

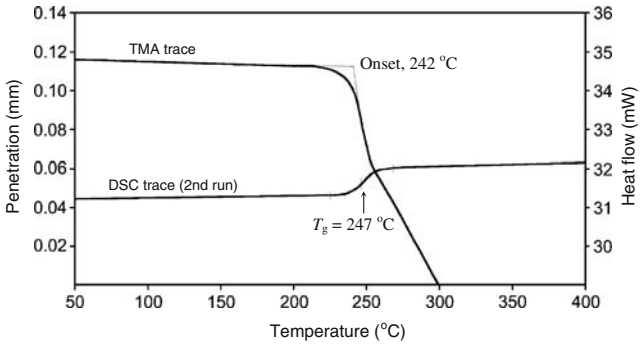


**Fig. 11** Typical DSC and TMA thermograms of the poly(ester-imide) *m*-**8d**: DSC, heating rate of 20 °C/min; TMA, heating rate of 10 °C/min and applied force of 10 mN

## Properties of poly(ester-imide)s

Morphological information of the poly(ester-imide)s was obtained by WAXD studies. The WAXD patterns of all the poly(ester-imide) samples prepared via chemical imidization route are also shown in Fig. 7. The poly(ester-imide)s *p*-**8a**, *p*-**8c**, *m*-**8a**, and *m*-**8c** derived from PMDA displayed some strong diffraction signals assignable to a semicrystalline polymer and did not afford a ductile film. The poly(ester-imide)s *p*-**8b**, *p*-**8d**, *m*-**8b**, and *m*-**8d** derived from 6FDA showed amorphous patterns. The copoly(ester-imide)s *p*-**8d** and *m*-**8d** could afford flexible and tough films. These films exhibited ultimate tensile strengths to break of 89–91 MPa, elongations to break of 7–8%, and initial moduli of 2.0–2.2 GPa (Table 1). However, the films of the homopoly(ester-imide)s *p*-**8b** and *m*-**8b** cracked upon creasing.

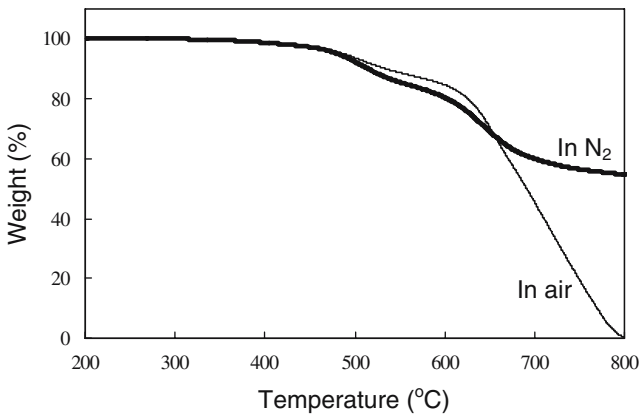


**Fig. 12** TGA curves of the poly(ester-imide) *m*-**8c** in nitrogen and air (heating rates of 20 °C/min)

The solubility properties of the poly(ester-imide)s are also reported in Table 4. In general, the semicrystalline polymers revealed a poor solubility. The homopoly(ester-imide)s *p*-**8a** and *m*-**8a** and copoly(ester-imide)s *p*-**8c** and *m*-**8c** derived from PMDA were insoluble in all of the organic solvents tested. The poly(ester-imide)s *p*-**8b** and *p*-**8d** derived from 6FDA were soluble in NMP, DMAc, DMF, and *m*-cresol at room temperature, but insoluble in DMSO. The poly(ester-imide)s *m*-**8b** and *m*-**8d** derived from 6FDA were soluble in all of the organic solvents tested.

As shown in Table 5, the poly(ester-imide)s, except polymer *p*-**8a**, showed clear $T_g$ values between 225 and 265 °C by DSC. A typical DSC thermogram, together with the TMA trace, for the representative poly(ester-imide) *m*-**8d** is illustrated in Fig. 11. The *p*-**8** series poly(ester-imide)s showed a higher $T_g$ as compared with the corresponding *m*-**8** series analogs. As can be seen from Table 5, the $T_s$ values of the flexible poly(ester-imide) films were recorded at 257°C for *p*-**8d** and 242°C for *m*-**8d,** which are comparable to their $T_g$ values determined by DSC.

The decomposition temperatures ($T_d$s) at 5 and 10% weight loss of the poly(ester-imide)s in nitrogen and air atmospheres determined from the original TGA thermograms are also summarized in Table 5. All of the poly(ester-imide)s exhibited good thermal and thermo-oxidative stabilities with insignificant weight losses up to temperatures of approximately 450 °C in both nitrogen and air atmospheres. The amounts of carbonized residues (char yields) at 800 °C in nitrogen for these poly(ester-imide)s were in the range 49–55 wt%. The $T_d$ values at 5% weight loss for the *p*-series poly(ester-imide)s ranged from 461 to 492 °C in nitrogen and 440 to 492 °C in air, which were lower than those of the analogous poly(ether-imide)s [38] because of the less stable ester groups. The $T_d$ values at 5% weight loss for the *m*-series poly(ester-imide)s were recorded in the range 461–481°C in nitrogen and 455–488 °C in air. Typical TGA curves of the poly(ester-imide)s *m*-**8c** are reproduced in Fig. 12. All of the poly(ester-imide)s seemed to exhibit a two-stage decomposition behaviour at elevated temperatures. The first stage of weight loss starting at around 350 °C might be attributed to the early degradation of the less stable ester groups.

## Conclusions

Two new bis(benzoyloxy)naphthalene-containing aromatic bis(ester-amine)s *p*-**2** and *m*-**2** have been successfully synthesized in high purity and good yields from the condensation reaction of 2,3-dihydroxynaphthalene with 4-nitrobenzoyl chloride and 3-nitrobenzoyl chloride, respectively, followed by subsequent catalytic hydrogen reduction of the intermediate dinitro compounds. The novel aromatic poly(ester-amide)s and poly(ester-imide)s having 2,3-linked naphthalene units have been successfully synthesized by the direct phosphorylation polyamidation and a conventional two-stage method, respectively, from the bis(ester-amine)s (*p*-**2** and *m*-**2**) and an equimolar mixture of the bis(ester-amine)s and 4,4′-oxydianiline with various aromatic dicarboxylic acids and dianhydrides. The poly(ester-amide)s *p*-**5a** and *p*-**5f** obtained from terephthalic acid (**4a**) were semicrystalline and showed less solubility. The homopoly(ester-imide)s *p*-**8a** and *m*-**8a** and copoly(ester-imide)s *p*-**8c** and *m*-**8c** derived from PMDA were insoluble in all of the organic solvents tested. Six copoly(ester-amide)s *p*-**5g-j** and *m*-**5i-j** and two copoly(ester-imide)s *p*-**8d** and *m*-**8d** could be cast into films. These polymers displayed good solubility, good film-forming capability, reasonable thermal stability, and moderate $T_g$ or $T_s$ values suitable for thermoforming processing. Investigation of the thermal degradation of the poly(ester-amide)s using IR spectroscopy indicated that ester groups are the thermal weak points of these polymers.

## References


1. Morgan PW (1979) Chemtech 9:316
2. Cassidy PE (1980) Thermally stable polymers. Marcel Dekker, New York
3. Yang HH (1989) Aromatic high-strength fibers. Wiley, New York
4. Yang HH (1993) Kevlar Aramid fiber. Wiley, New York
5. Wilson D, Stenzenberger HD, Hergenrother PM (eds) (1990) Polyimides, Blackie, Glasgow and London
6. Ghosh MK, Mittal KL (eds) (1996) Polyimides: fundamentals and applications, Marcel Dekker, New York
7. Hsiao S-H, Yang C-P, Fan J-C (1994) J Polym Res 1:345
8. Maglio G, Palumbo R, Vignola MC (1995) Macromol Chem Phys 196:2775
9. Hsiao S-H, Yu C-H (1996) J Polym Res 3:247
10. Tamai S, Yamaguchi A, Ohta M (1996) Polymer 37:3683
11. Hsiao S-H, Huang P-C (1997) Macromol Chem Phys 198:4001
12. Hsiao S-H, Huang P-C (1997) J Polym Res 4:189
13. Eastmond GC, Paprotny J, Irwin RS (1999) Polymer 40:469
14. Li Q, Fang X, Wang Z, Gao L, Ding M (2003) J Polym Sci, Part A: Polym Chem 41:3249
15. Hsiao S-H, Lin K-H (2004) Polymer 45:7877
16. Hsiao S-H, Lin K-H (2005) J Polym Sci, Part A: Polym Chem 43:331
17. Imai Y (1995) High Perform Polym 7:337
18. Hsiao S-H, Li C-T (1998) Macromolecules 31:7213
19. Eastmond GC, Gibas M, Paprotny J (1999) Eur Polym J 35:2097
20. Liaw D-J, Liaw B-Y, Yang C-M (2001) Macromol Chem Phys 201:1866
21. Hsiao S-H, Huang T-L (2004) J Polym Res 11:9
22. Yang C-P, Su Y-Y (2005) J Polym Res 12:17
23. Hsiao S-H, Yang C-P, Chen C-W (2005) J Polym Res 12:289
24. Chung C-L, Tzu T-W, Hsiao S-H (2006) J Polym Res 13:495
25. Imai Y (1996) React Funct Polym 30:3
26. Chern Y-T, Shiue H-C (1997) Macromolecules 30:4646

27. Chern Y-T, Shiue H-C (1997) Macromolecules 30:5766
28. Liaw D-J, Liaw B-Y, Jeng M-Q (1998) Polymer 39:1597
29. Li F, Fang S, Ge JJ, Honigfort PS, Chen J-C, Harris FW, Cheng SZD (1999) Polymer 40:4571
30. Li F, Ge JJ, Honigfort PS, Fang S, Chen J-C, Harris FW, Cheng SZD (1999) Polymer 40:4987
31. Wu S-C, Shu C-F (2003) J Polym Sci, Part A: Polym Chem 41:1160
32. Liou G-S, Fang Y-K, Yen H-J (2007) J Polym Res 14:147
33. Takekoshi T, Kochanowski JE, Manello JS, Webber MJ (1986) J Polym Sci, Polym Symp 74:93
34. Eastmond GC, Paprotny J (1996) React Funct Polym 30:27
35. Tamai S, Yamaguchi A, Ohta M (1996) Polymer 37:3686
36. Hsiao S-H, Chen Y-J (2002) Eur Polym J 38:815
37. Yang C-P, Chen W-T (1993) Makromol Chem 194:1595
38. Yang C-P, Chen W-T (1993) Macromolecules 26:4865
39. Hsiao S-H, Yang C-P, Chu K-Y (1997) Macromolecules 30:165
40. Hsiao S-H, Chu K-Y (1997) Macromol Chem Phys 198:819
41. Hsiao S-H, Yang C-P, Chu K-Y (1997) Macromol Chem Phys 198:2153
42. Hsiao S-H, Liou G-S (1998) Macromol Chem Phys 199:2321
43. Yang C-P, Hsiao S-H, Yang C-C (2004) J Polym Res 11:23
44. Hsiao S-H, Chang C-F (1996) Macromol Chem Phys 197:1255
45. Eastmond GC, Paprotny J (1997) J Mater Chem 7:1321
46. Eastmond GC, Paprotny J, Irwin RS (1999) Polymer 40:469
47. Eastmond GC, Paprotny J (2004) Polymer 45:1073
48. Yamazaki N, Matsumoto M, Higashi F (1975) J Polym Sci, Polym Chem Ed 13:1373